Emerging inverse energy transfer in superfluid helium-4 vortex reconnections

P. Z. Stasiak, A. Baggaley, and C.F. Barenghi
School of Mathematics, Statistics and Physics, Newcastle University, Newcastle upon Tyne, NE1 7RU, United Kingdom

G. Krstulovic
Université Côte d'Azur, Observatoire de la Côte d'Azur, CNRS,Laboratoire Lagrangre, Boulevard de l'Observatoire CS 34229 - F 06304 NICE Cedex 4, France

L. Galantucci
Istituto per le Applicazioni del Calcolo "M. Picone" IAC CNR, Via dei Taurini 19, 00185 Roma, Italy
(Dated: September 19, 2024)

Lorem ipsum dolor sit amet, consectetuer adipiscing elit. Etiam lobortis facilisis sem. Nullam nec mi et neque pharetra sollicitudin. Praesent imperdiet mi nec ante. Donec ullamcorper, felis non sodales commodo, lectus velit ultrices augue, a dignissim nibh lectus placerat pede. Vivamus nunc nunc, molestie ut, ultricies vel, semper in, velit. Ut porttitor. Praesent in sapien. Lorem ipsum dolor sit amet, consectetuer adipiscing elit. Duis fringilla tristique neque. Sed interdum libero ut metus. Pellentesque placerat. Nam rutrum augue a leo. Morbi sed elit sit amet ante lobortis sollicitudin. Praesent blandit blandit mauris. Praesent lectus tellus, aliquet aliquam, luctus a, egestas a, turpis. Mauris lacinia lorem sit amet ipsum. Nunc quis urna dictum turpis accumsan semper.

Introduction.— ....

Main results.— In this Letter, we use the Schwarz model [1] to evolve vortex filaments $\mathbf{s}(\xi, t)$, where ξ is the natural parametrisation of vortex lines, also known as the arclength. The normal fluid is coupled via the mutual friction force $\mathbf{f}_{ns}$ in a self-consistent manner using a recently developed technique in Ref. [2]. Further details of the method are outlined in Ref. [3] and the corresponding Supplementary Materials. We set two pairs of orthogonal vortices, where each vortex in the pair has the same circulation $\pm\kappa$, to preserve superfluid periodicity along the boundaries, and we consider two finite temperatures, $T = 1.9K$ and $T = 2.1K$. Vortex pairs are seperated by distance D_ℓ, and each vortex within each pair is seperated by distance d_ℓ, such that $D_\ell \ll d_\ell$, see Fig. 1. The seperation of scales ensures that the dynamics in the vicinity of the reconnection are dominated by local interactions, and that far-reaching contributions from the other vortex pair are negligent. The normal fluid is initally quiescent, and evolves according to a classical Navier-Stokes equation

$$\frac{\partial \mathbf{v}}{\partial t} + (\mathbf{v}\cdot\nabla)\mathbf{v} = -\nabla\left(\frac{p}{\rho_n}\right) + \nu_n\nabla^2\mathbf{v} + \frac{\mathbf{F}_{ns}}{\rho_n} \quad (1)$$

where $\mathbf{v}$ denotes the normal fluid velocity, p is the pressure, ρ_n is the normal fluid density, ν_n is the kinematic viscosity and $\mathbf{F}_{ns}$ is the mutual friction coupling, arising from the relative motion between the normal fluid and superfluid vortices $\mathbf{F}_{ns} \propto |\mathbf{v}_l - \mathbf{v}|$ where $\mathbf{v}_l$ is the velocity of vortex lines. The generation of the force is highly localised in space, at microscopic length scales on the order of the vortex core radius $\sim a_0$, and $\Delta x \gg a_0$, where Δx is a typical grid discretisation. Abrupt changes in the topology of vortex lines, such as during vortex reconnections, form highly curved cusps and strongly inject vorticity (see Fig. 1), since $|\mathbf{v}_l - \mathbf{v}| \approx |\mathbf{v}_l| \propto \zeta$ in the first approximation, where ζ is the curvature of vortex lines.

In this way, energy is injected into the normal fluid at the small length scales in a natural way in the absence of external property, an intrinsic and unique feature of quantum fluids. The injection of energy is clear in the kinetic energy spectrum E_k which is shown in in Fig. 2, at wavenumbers $k > 10$ a vast increase can be observed $E_k(t \approx t_0)/E_k(t \ll t_0) \sim 10^2$, evidence of very strong energy injection. Remarkably, in the post reconnection regime E_k appears to increase when k is small, and decay at large values of k, suggesting a possible mechanism by which energy generated at small length scales is transferred to larger scales. The energy spectrum E_k evolves according to the balance sources/sinks and internal transfers,

$$\frac{\partial E_k}{\partial t} = T_k - D_k + I_k \quad (2)$$

where T_k is the spectral kinetic energy transfer function, $D_k = 2\nu_n k^2 E_k$ is the dissipation spectrum and $I_k = \mathrm{Re}(\hat{\mathbf{F}}_{ns}(\mathbf{k})\cdot\hat{\mathbf{v}}^*(\mathbf{k}))$ is the injection spectrum due to the mutual friction $\mathbf{F}_{ns}$. The injection spectrum I_k as shown in Fig. 3a again shows that the injection of energy covers primarily the high k range, but is not limited to a thin band of injection. In fact, the energy flux $\Pi_E(k) = \int_k^\infty T_k dk$ as shown in Fig. 3b asserts a hallmark feature of inverse energy cascades, typical in 2D isotropic turbulence. A flux of $\Pi_E(k) < 0$ implies a negative flux of energy from small to large k, i.e. an inverse transfer of energy. The effect of kinetic energy transferral to large length scales results in the creation of large scale structures, evident in the evolution of the integral length scale

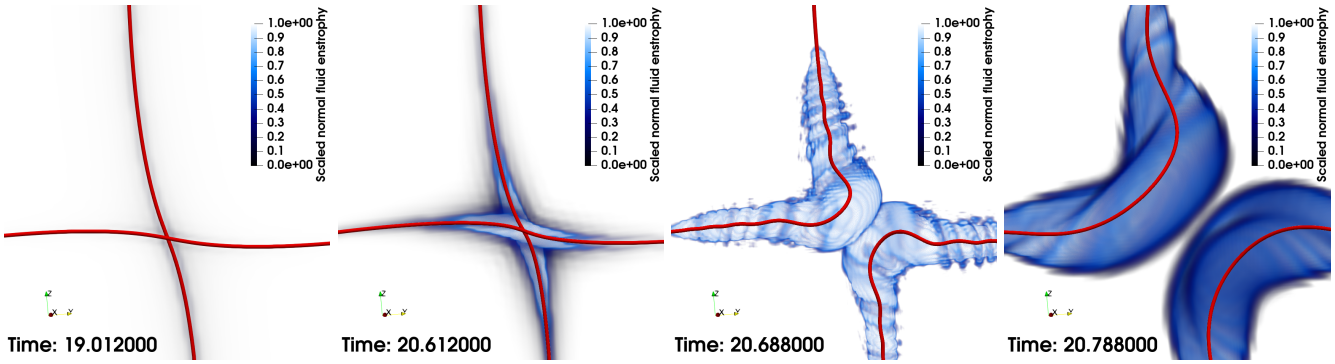

FIG. 1: 3D rendering of an orthogonal vortex configuration, undergoing a vortex reconnection. The red tube represents a superfluid vortex, where the radius has been greatly exaggerated for visual purposes, and the blue volume rendering represents the scaled normal fluid enstrophy $\boldsymbol{\omega}^2/\boldsymbol{\omega}^2_{max}$.

$\mathcal{L}_E$, where

$$\mathcal{L}_E = \frac{\pi}{2\langle \mathbf{v}'^2 \rangle} \int_0^\infty \frac{E_k}{k} dk \tag{3}$$

and $\langle \mathbf{v}'^2 \rangle$ represents the turbulent kinetic energy. In the inset of Fig. 3b, $\mathcal{L}_E$ steadily increases in the post-reconnection region, implying a generation of large scale structure.

In order to explain the inverse energy transfer mechanism, we follow recent work in classical fluids outlined in Refs. [4, 5], where it is even possible to sustain an inverse energy cascade under a helical forcing applied at all length scales. Typically, velocity coefficients $\hat{\mathbf{v}}(\mathbf{k})$ can be decomposed into their helical modes, where $\hat{\mathbf{v}}(\mathbf{k}) = v^+(\mathbf{k})\mathbf{h}^+(\mathbf{k}) + v^-(\mathbf{k})\mathbf{h}^-(\mathbf{k})$ and satisfies $\mathbf{k}\cdot\hat{\mathbf{v}}(\mathbf{k}) = 0$, where $\mathbf{v}^\pm$ are complex scalars and $\mathbf{h}^\pm(\mathbf{k})$ are the two eigenvectors of the curl operator, such that $i\mathbf{k}\times\mathbf{h}^\pm(\mathbf{k}) = \pm k\mathbf{h}^\pm(\mathbf{k})$. To explain the inverse energy transfer in terms of helical modes, we show that in fact the driving force, which in our case is a punctuated burst due to superfluid vortex reconnections, is of a helical nature. The mutual friction modes $\hat{\mathbf{F}}_{ns}(\mathbf{k})$ are not incompressible, and so we take the projection of the modes orthogonal to the wavenumber $\mathbf{k}$,

$$\hat{\mathbf{f}}(\mathbf{k}) = \hat{\mathbf{F}}_{ns}(\mathbf{k}) - \frac{(\hat{\mathbf{F}}_{ns}(\mathbf{k})\cdot\mathbf{k})}{k^2}\mathbf{k}. \tag{4}$$

The projected modes $\hat{\mathbf{f}}(\mathbf{k})$ are then decomposed into helical modes $\hat{\mathbf{f}}(\mathbf{k}) = f^+\mathbf{h}^+(\mathbf{k}) + f^-\mathbf{h}^-(\mathbf{k})$. The ratio of the two helical modes $|f^+|^2/|f^-|^2$ are shown in Fig. 4. At reconnection time t_0, the ratio is much larger, indicating a clear inbalance that favours the injection of positive helical modes. In the same way, helicity modes $\hat{\mathcal{H}}(\mathbf{k})$ can be decomposed,

$$\hat{\mathcal{H}}(\mathbf{k}) = k(E^+(\mathbf{k}) - E^-(\mathbf{k})) = \mathcal{H}^+ + \mathcal{H}^- \tag{5}$$

where $E^\pm = \frac{1}{2}|\mathbf{v}^\pm(\mathbf{k})|^2$ are the helical energy modes. The evolution of the ratio $\mathcal{H}^+/\mathcal{H}^-$ is shown in Fig. 5. The sharp increase at reconnection time t_0 is evidence of a large influx of positive helical modes as a result of the vortex reconnection, which is in agreement with the conditions to facilitate an inverse energy transfer by a helical injection. Finally, as observed in Ref. [5], it is necessary for the forcing to cover the entire spectrum of k, which from Fig. 3a, it is evident that this indeed the case.

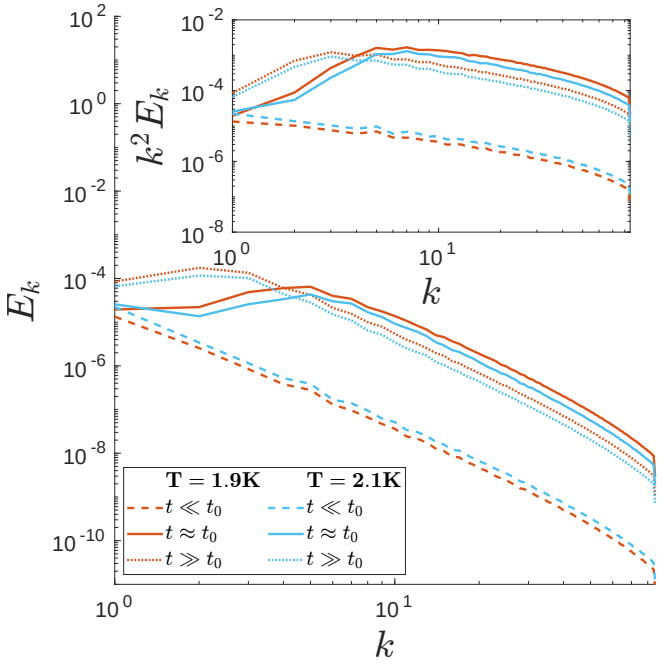

FIG. 2: Normal fluid kinetic energy spectrum E_k before reconnection (dashed lines), at reconnection (solid lines) and after reconnection (dotted lines) for $T = 1.9K$ and $T = 2.1K$. *Inset:* Dissipation spectrum $D_k/2\nu_n = k^2E_k$ at the same snapshots in time.

Closing remarks.— ...

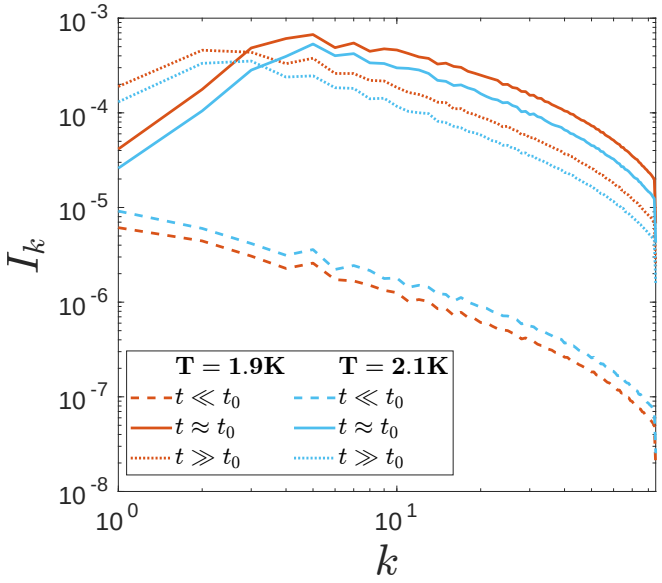

(a)

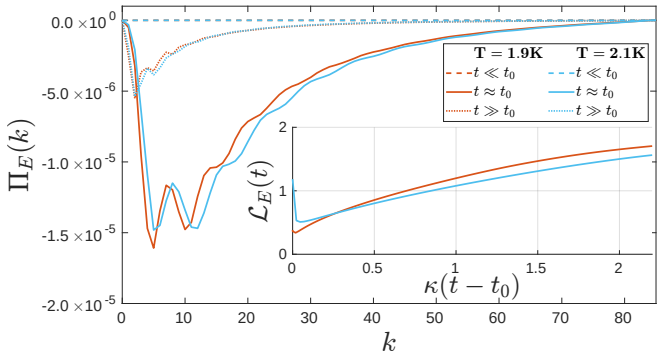

(b)

FIG. 3: *Top:* Mutual friction injection spectrum I_k. *Bottom:* Spectral normal fluid kinetic energy flux Π_E. *Inset:* Post reconnection evolution of the integral length scale $\mathcal{L}_E$.

[1] KW. Schwarz, Three-dimensional vortex dynamics in superfluid ^{4}He, Phys. Rev. B **38**, 2398 (1988).

[2] L. Galantucci, A. W. Baggaley, C. F. Barenghi, and G. Krstulovic, A new self-consistent approach of quantum turbulence in superfluid helium, Eur. Phys. J. Plus **135**, 547 (2020).

[3] Punctuated energy injection in superfluid helium-4 vortex reconnections.

[4] L. Biferale, S. Musacchio, and F. Toschi, Inverse Energy Cascade in Three-Dimensional Isotropic Turbulence, Phys. Rev. Lett. **108**, 164501 (2012).

[5] F. Plunian, A. Teimurazov, R. Stepanov, and M. K. Verma, Inverse cascade of energy in helical turbulence, J. Fluid Mech. **895**, A13 (2020).

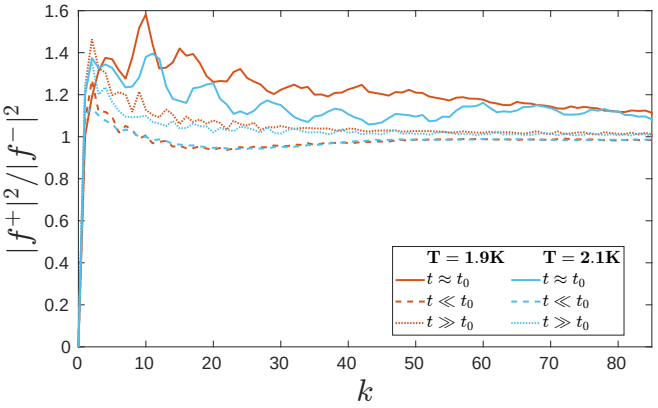

FIG. 4: The ratio of the projected helical mutual friction modes $f^+(k)$ and $f^-(k)$

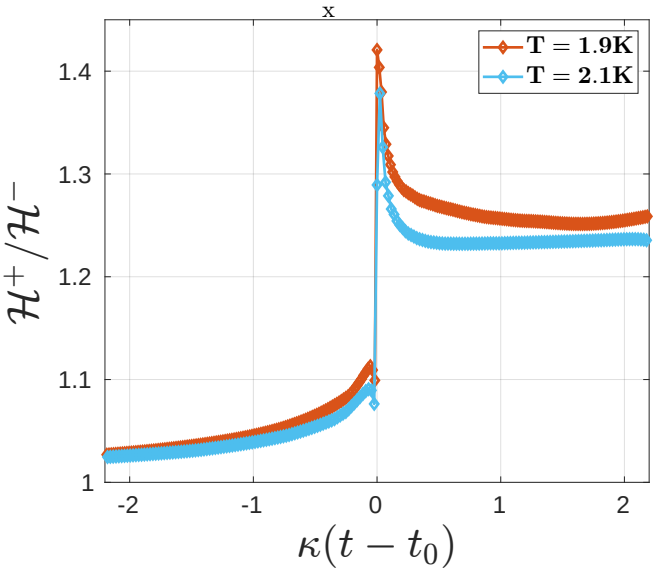

FIG. 5: Balance of helical helicity modes $\mathcal{H}^+$ and $\mathcal{H}^-$.